Progress In Electromagnetics Research C, Vol. 131, 171–184, 2023

Dual Cost Function Model Predictive Control for PMSM

Dingdou Wen, Wenting Zhang, Zhe Li, Zhongjian Tang, Yang Zhang, and Yun Ling*

Abstract—In model predictive current control (MPCC), in order to reduce the switching frequency, the number of switching changes is introduced into the cost function. But it will lead to the complexity of weight coefficient adjustment. To solve the problem, a dual cost function model predictive control (DCF-MPC) strategy for permanent magnet synchronous motor (PMSM) is proposed. First, the dual cost function is established, and the cost function g_1 first screens out the combination of two or three voltage vectors which minimizes the current steady-state error. Then, the cost function g_2 selects the voltage vector combination that minimizes the number of switching changes from the selected voltage vector combinations in g_1 as the optimal voltage vector combination. Finally, the experiment shows that compared with the traditional single cost function, the proposed method eliminates the weight coefficient of MPCC, simplifies the system structure, and reduces the amount of calculation. Moreover, it suppresses the stator current ripple, reduces the harmonic content of three-phase current, and has better steady-state and dynamic performance under different working conditions.

1. INTRODUCTION

With the improvement of rare earth permanent magnet material performance and the gradual reduction of cost, as well as the development of power electronics technology, permanent magnet synchronous motor (PMSM) has been extensively used in various industrial applications varying from electric vehicles, ships, computer numerical control (CNC) machine tools to aerospace industry because of its high density of power, small size, simple structure, and strong reliability [1].

Rodriguez et al. first proposed a finite control set model predictive control (FCS-MPC) method for two-level inverters [2, 3]. As a high performance control strategy, it has gained more and more attention because of its simple principle, fast response speed, flexible control of various system variables, and being suitable for PMSM control applications. Classical control strategies are divided into Direct Torque Control (DTC) [4] and Field-Oriented Control (FOC) [5]. DTC has excellent dynamic performance, but it cannot meet the needs of industrial high efficiency because of its large torque ripple. In [6], the vector synthesis method is used to reduce torque ripple, but the switching frequency is increased, resulting in heat loss of the converter. Reference [7] combines model predictive current control with dual vector control to reduce current ripple effectively and make MPC have good dynamic and static performance. In order to maintain the good dynamic advantage of MPC, while taking advantage of its ability to handle multiple control objectives and system constraints, reference [8] introduces converter switching frequency into the control strategy, reducing switching loss but increasing torque ripple. In [9], aiming at the problem of poor performance caused by the bandwidth limitation of PMSM current loop under low carrier wave ratio conditions, the switching frequency of the converter is introduced as an additional term into the cost function to reduce the switching loss and improve the static performance of the motor. The switching frequency of the inverter in [10] does not introduce constrained condition, which leads to increased loss of switching devices, severe heating, and even affects the service life of

Received 15 January 2023, Accepted 14 March 2023, Scheduled 27 March 2023
* Corresponding author: Yun Ling (896800286@qq.com).
The authors are with the College of Electrical and Information Engineering, Hunan University of Technology, Zhuzhou 412007, China.

switching devices. Therefore, it is necessary to introduce switching times as constraint term in the cost function to reduce switching frequency, decrease the system losses, and further improve the stability and reliability of PMSM.

In order to meet different control requirements, constraints such as inductance voltage and current ripple can be introduced into the cost function, or a new cost function can be designed to improve the performance of the motor control system. According to different controlled variables, the cost function can be divided into two types: weight coefficient not included [11] and weight coefficient included [12, 13].

In the MPC of PMSM, multi-objective optimal cooperative control relies on the selection of weight factors. Too large or too small weight factors will lead to system instability, and the design of weight coefficients lacks theoretical guidance. Usually, rating method, trial and error method, and branch and bound method are used. The weight factors determined by these methods are single and cannot meet the requirements of motors under different working conditions. Therefore, the setting of weight factors has always been a research hotspot and difficulty in the academic community. Some scholars have carried out a series of studies from the online tuning strategy. In [14], a method based on artificial neural network is proposed to solve the problem of weight factors selection, which enables the cost function to obtain different weight factors under different operating conditions. However, it relies on a large amount of data and requires a large amount of calculation. In [15], a method is proposed to adjust the weight factor with the change of the amplitude and phase angle reference of the voltage, effectively reducing the current ripple, but increasing computational complexity. In [16], a fuzzy logic control method to adjust the weight factor dynamically under the steady state and transient state of the motor is proposed to achieve low switching frequency, but the weight factor cannot be ensured to be globally optimal. In [17], a genetic algorithm is used to solve the problem of weight factor allocation in multiple control objectives, but it relies too much on motor parameters. In [18], the weight factor is adjusted dynamically according to different operating conditions through adaptive method, and the system control performance is improved, but whether the weight factor is optimal is not verified. In [19], the traditional Gaussian distribution model is used to realize the self-tuning of the weight factor in the cost function, which reduces the switching frequency of the system and circumvents the design problem of weight factor, but the calculation is heavy.

The online tuning method solves the problem that the weight factor remains unchanged in the control, but the calculation is large. When the motor runs for a long time, the motor parameters will be changed, and the control system performance will decline. To address this problem, some scholars have carried out research on eliminating the weight factor. In [20], torque error and flux linkage error are proposed as two cost functions, and the respective values are ranked separately. The average value of two cost function serial numbers is taken, and the voltage vector that minimizes the average value is applied. In [21], a control method based on logic operation is proposed for model predictive torque. The flux linkage, torque, and switching frequency in the cost function are ranked, and the serial numbers are added to select the voltage vector that minimizes the sum of the serial numbers. This method eliminates the weight factor and reduces the calculation, but ignores the dimension problem of these three items. Reference [22] proposes an improved model predictive torque control strategy. The weight factor of stator flux and the restriction of unit difference between torque and flux in traditional MPTC are eliminated by converting torque and flux amplitude into stator flux reference vector, but the flux change caused by magnetic field weakening is not considered, and observers are added in the prediction process, which increases the complexity of control. In the model predictive control of induction motor in [23], according to the relationship between electromagnetic torque and flux amplitude, the cost function is converted into stator flux vector, which eliminates the weight coefficient and improves the motor performance. In [24], two cost functions, torque and flux, are set, and a penalty term is introduced into the flux cost function. The two cost functions operate in parallel. The optimal voltage vector is selected through a predetermined algorithm, which has better robustness, but ignores the difference in dimension and amplitude between additional terms and error terms.

Therefore, this paper proposes a novel DCF-MPC method to obtain good control performance. The contributions of this paper are summarized as follows:

(i) In the proposed method, the voltage vector combinations are screened twice, and switching times of voltage vector are needed to be calculated only two or three times, which avoids calculating the switching times of all voltage vector combinations and reduces the amount of calculation.

(ii) The proposed method uses two cost functions to eliminate the weighting factor.

(iii) Compared with the traditional single cost function, the proposed method has better robustness, steady-state characteristics, and dynamic characteristics.

The rest of this paper is as follows. Section 2 introduces the model. Section 3 analyzes the MPC of single cost function. Section 4 focuses on the DCF-MPC. Section 5 shows the fine test results of DCF-MPC compared to another plan. Finally, Section 6 briefly summarizes this paper.

2. MATHEMATICAL MODEL OF PMSM

In this paper, the surface-mounted PMSM is taken as the research object, and the magnetic flux linkage, iron saturation, hysteresis loss, and eddy current are assumed to be negligible [25].

The stator current equation of PMSM in a *d-q* coordinate system is expressed as:

$$\frac{\mathrm{d}i_d}{\mathrm{d}t} = \left(u_d - R_k i_d + \omega_e L_s i_q\right)/L_s \tag{1}$$

$$\frac{\mathrm{d}i_q}{\mathrm{d}t} = \left(u_q - R_s i_q - \omega_e L_s i_d - \omega_e \psi_f\right)/L_s \tag{2}$$

where u_d, u_q, i_d, i_q are the voltages and currents of the *d-q* axis, respectively. R_s is the stator resistance, L_s the stator inductance, ψ_f the permanent magnet flux linkage, and w_e the electrical angular velocity.

Using the first-order Eulerian discretization method, the discretizations of (1) and (2) are expressed as:

$$i_d(k+1) = i_d(k) + T_s[u_d(k) - R_s i_d(k) + e_d(k)]/L_s \tag{3}$$

$$i_q(k+1) = i_q(k) + T_s[u_q(k) - R_s i_q(k) + e_q(k)]/L_s \tag{4}$$

$$e_d(k) = \omega_e(k) L_s i_q(k) \tag{5}$$

$$e_q(k) = -\omega_e(k) L_s i_d(k) - \omega_e(k)\psi_f \tag{6}$$

where $i_d(k)$ and $i_q(k)$ are the *d-q* axis current components at the time, respectively. $i_d(k+1)$ and $i_q(k+1)$ are the *d-q* axis current components at the next sampling time, respectively. $e_d(k)$ and $e_q(k)$ are the *d-q* axis back electromotive force (EMF) at the time, respectively. T_s is the sampling time.

3. SINGLE COST FUNCTION MPC STRATEGY

Since the two-level inverter can generate 6 effective voltages and 2 zero vectors, it can synthesize $7 * 7$ combinations of two voltage vectors, which requires a large amount of calculation.

In this paper, each sector is designed to use a combination of 1 effective vector and 1 zero vector or 2 effective vectors. The deadbeat principle is used to allocate the time of 2 voltage vectors in a sampling period in the q axis. Since the sequence of the 2 vectors in a sampling period does not affect the working time of the 2 vectors, it is only necessary to select the optimal voltage vector combination from 21 pairs of voltage vector combinations.

The optimal combination is selected from 21 pairs of voltage vector combinations, so the selection range of voltage vector is much wider than that of single vector model predictive control. In the process of optimal voltage vector combination, the action time of 2 voltage vectors (V_i and V_j) in the combination is considered, which ensures that the selected voltage vector combination is optimal and reduces the calculation amount from the source.

Implementation steps are as follows:

1) Calculation of duty cycle

The duty cycle is calculated by the deadbeat of the q-axis current, that is, in a single T_s, by allocating the action time of 2 voltage vectors, and i_q is equal to i_q^* at the moment of $(k+1)T_s$, namely:

$$i_q(k+1) = i_q(k) + s_i t_i + s_j(T_s - t_i) = i_q^* \tag{7}$$

According to (7), the working time of the first voltage vector is as follows:

$$t_i = [i_q^* - i_q(k) - s_j T_s]/(s_i - s_j) \tag{8}$$

Then the second vector working time is as follows:

$$t_j = T_s - t_i \tag{9}$$

2) Calculation of the i_q slope

According to (1) and (2), the slope of i_q under the action of 2 voltage vectors is as follows:

$$s_i = \left.\frac{\mathrm{d}i_q}{\mathrm{d}t}\right|_{u_q=u_{qi}} = \frac{u_{qi}}{L_s} + \left(-R_s i_q - \omega_r L_s i_d - \omega_r \psi_f\right)/L_s \tag{10}$$

$$s_j = \left.\frac{\mathrm{d}i_q}{\mathrm{d}t}\right|_{u_q=u_{qj}} = \frac{u_{qj}}{L_s} + \left(-R_s i_q - \omega_r L_s i_d - \omega_r \psi_f\right)/L_s \tag{11}$$

where u_{qi} and u_{qj} are the q-axis components of the stator voltage corresponding to V_i and V_j, respectively.

3) Calculation of predicted current

Through (8) and (9), the action time of each group of voltage vectors is preassigned, while using the mathematical model to predict the current, the action time of voltage vectors is considered to obtain the corresponding u_d and u_q, namely:

$$u_d = [t_i u_{di} + (T_s - t_i)u_{dj}]/T_s \tag{12}$$

$$u_q = [t_i u_{qi} + (T_s - t_i)u_{qj}]/T_s \tag{13}$$

The current prediction value is obtained by bringing u_d and u_q into (3) and (4). The coordinates of the corresponding voltage vector endpoints for each switching state in the α-β coordinate system are shown in Table 1.

Table 1. Switch status.

$S_{abc} = (S_a\ S_b\ S_c)$	u_α	u_β
(0 0 0)	0	0
(0 0 1)	$-U_{DC}/3$	$-U_{DC}/3$
(0 1 0)	$-U_{DC}/3$	$U_{DC}/\sqrt{3}$
(0 1 1)	$-2 * U_{DC}/3$	0
(1 0 0)	$2 * U_{DC}/3$	0
(1 0 1)	$U_{DC}/3$	$-U_{DC}/\sqrt{3}$
(1 1 0)	$U_{DC}/3$	$U_{DC}/\sqrt{3}$
(1 1 1)	0	0

4) Selection of optimal voltage vector combination

Taking the predicted current values obtained from (3) and (4) into the cost function in turn, the voltage vector combination that minimizes the cost function value is selected. Model predictive control is used to consider multiple nonlinear control objectives in the cost function. In this paper, reducing the switching frequency of the converter is taken as one of the control objectives, so that the system can achieve better control effect than the vector control and reduce the current ripple. That is, based on the single cost function (SCF) model predictive current control with switching frequency as an additional term, a new cost function is constructed:

$$g = |i_d^* - i_d(k+1)|^2 + |i_q^* - i_q(k+1)|^2 + \lambda\left(|S_1^k - S_2^k| + 2 * |S_1^k - S_1^{k-1}|\right) \tag{14}$$

where λ is the weighting factor, S_1^k the first vector of the voltage vector combination selected in the current control cycle, S_2^k the second vector of the vector combination selected in the current control cycle, and S_1^{k-1} the switch state at the end of the vector combination selected in the previous control cycle.

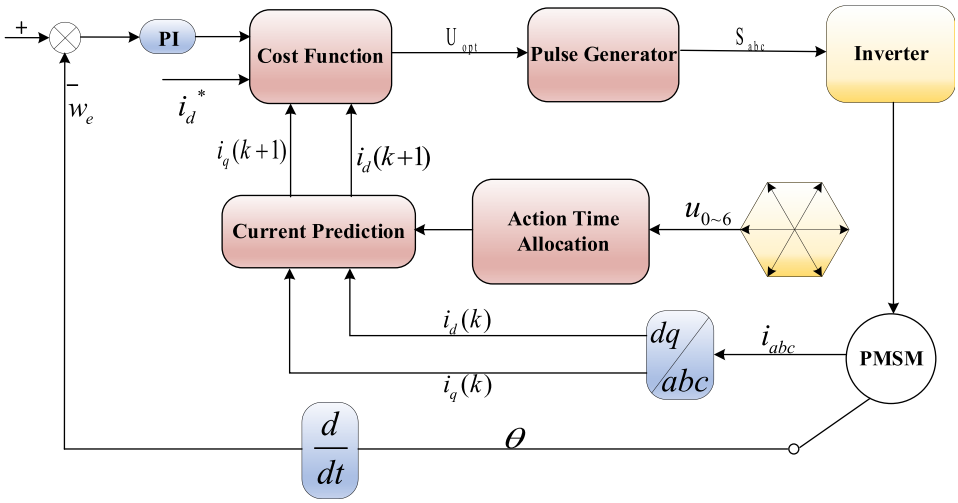

Figure 1. The principle block diagram of SCF-MPC.

The principle block diagram of SCF- MPC is shown in Figure 1.

5) Allocation of vector action time

The switching frequency can be reduced to a certain extent through the selection of zero vector. For example, if $u_5(101)$ is combined with zero vector (000 or 111), and zero vector (111) is selected, the switch only needs to be changed once, but selecting zero vector (000) requires changing the switch twice. Therefore, only zero vector (111) can be selected to reduce switching frequency. The voltage vector diagram is shown in Figure 2.

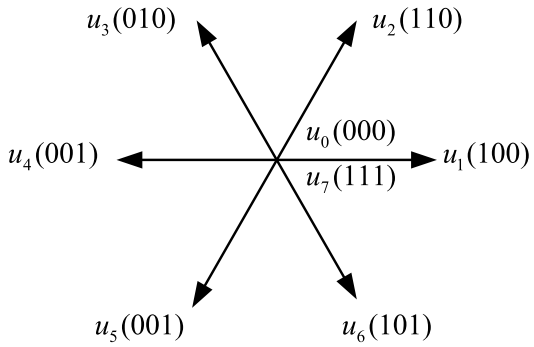

Figure 2. The voltage vector diagram.

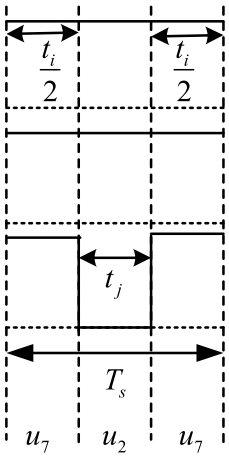

Figure 3. The allocation of turn-on time of the three-phase bridge.

To reduce the current harmonics, PWM symmetrical wave generation is used. When the last switching state of the previous cycle is (101), the combination of voltage vectors of (110) and (111) is selected, and the allocation of turn-on time of the three-phase bridge arm is shown in Figure 3. Since the number of switching changes between vector combinations is fixed, and the number of switching changes from the last switching state (101) to (111) in the previous cycle is the smallest, $u_7(111)$ is selected as the first voltage applied in this cycle, which further reduces the switching frequency.

4. MPC CONTROL STRATEGY OF DUAL COST FUNCTION

In (14), the weight factor λ requires repeated simulations and experiments to optimize, and the amount of calculation is large, which is not conducive to the practical application of MPC.

In this paper, a dual cost function (DCF) model predictive control strategy is proposed. Through the two cost functions g_1 and g_2 in (15) and (16), the voltage vector combination is screened in turn, and the optimal voltage vector combination is finally obtained. When SCF is optimized in the cost function, it is necessary to calculate the number of changes of 21 groups of voltage vector combination switches. In DCF, because two cost functions g_1 and g_2 are used to screen in turn, if g_1 screens out too many voltage vector combinations, the calculation amount cannot be effectively reduced. If the combination of voltage vectors screened by g_1 is too small, the switching frequency cannot be reduced. Therefore, how many voltage vector combinations are screened from g_1 is the key. After analysis, two groups of voltage vectors (DCF2) or three groups of voltage vectors (DCF3) are first selected from g_1, and then they are screened again. The calculation times are optimal. DCF2 only needs to count the number of switching changes twice, while DCF3 needs to count the number of switching changes three times. Therefore, compared to SCF, DCF once again reduces the amount of calculation in the optimization process. Meanwhile, by introducing a fixed weight factor into SCF, the dynamic balance between the stator current and switching frequency cannot be achieved. The DCF can not only ensure the control performance of the system, but also significantly reduce the calculation amount based on the switching frequency change of the system, and eliminate the weight factor. Finally, the cost function g_2 further screens the number of switching changes of the voltage vector combination screened by the cost function g_1 to ensure that the stator current error of the screened voltage vector combination is minimized, and the switching frequency is appropriate.

Implementation steps are as follows:

1) Design of the cost function g_1

The cost function g_1 is expressed as:

$$g_1 = |i_d^* - i_d(k+1)|^2 + |i_q^* - i_q(k+1)|^2 \tag{15}$$

By substituting (3) and (4) into (15), the voltage vector combination that minimizes the cost function g_1 is obtained.

g_1 uses the sum of the square of the stator current reference value and the given value error to track the stator current change, which can more accurately track the current change.

2) Design of the cost function g_2

The additional term of switching frequency is introduced into the control strategy, and the cost function g_2 of switching change times is designed:

$$g_2 = |S_1^k - S_2^k| + 2 * |S_1^k - S_1^{k-1}| \tag{16}$$

The action time of the two vectors in the voltage vector combination is evenly distributed in a control cycle to make the PWM waveform symmetrical. Therefore, the number of switching changes between vector combinations needs to be calculated twice, and the difference with the last switching state of the inverter in the previous cycle is added. In g_2, the number of switching changes is introduced as the secondary term, which avoids the complex design of weight factors.

3) MPC of dual cost function

Firstly, the first cost function g_1 is calculated in the voltage vector combination generated by each inverter through (15). Then the combination of two voltage vectors or three voltage vectors that minimizes g_1 is selected. Finally, the second cost function g_2 is used to screen out the combination of voltage vectors that minimize g_2.

g_2 is to calculate the total number of switching changes in each voltage vector combination. When the number of switching changes is an integer, there may be the same number of switching changes in two voltage vector combinations, and both of them minimize g_2. For example, the last switching state of the last cycle is (010), while the switching times of the vector combination of (110) and (101) and that of (011) and (000) are 6 times. In this case, in order to select the optimal voltage vector, it is necessary to select again the combination of voltage vectors that makes g_1 smaller.

4) Comparative analysis of DCF2 and DCF3

Compared with DCF, because the weight factor of SCF is fixed, the dynamic characteristics of the control system are poor, and the optimal voltage vector screened by SCF cannot be ensured to be globally optimal, resulting in an increase of current ripple. However, under the action of two cost functions, DCF avoids the weight factor and does not need to consider the weight analysis between the stator current error and the number of switching changes when the motor changes dynamically. Through double-layer screening, the stator current error and the number of switching changes of the optimal voltage vector combination are controlled within a reasonable range. Therefore, DCF has better dynamic and steady state performance.

In DCF design, DCF2 and DCF3, can not only ensure that the cost function can meet the requirements of low switching frequency and reduce calculation, but also avoid the problem of small current ripple and large switching loss in the control system. The differences between DCF2 and DCF3 are as follows:

(1) Compared with DCF3, DCF2 reduces the number of calculation times of voltage vector combination by one time and has lower calculation amount. The default motor parameters remain unchanged for a short period of time, reducing the impact of motor parameter changes on the steady-state and dynamic performance of the control system.

(2) For DCF2, it is only necessary to screen two groups of voltage vector combinations in g_1, and simply compare the switching times of the two groups of voltage vector combinations in g_2 to obtain the optimal voltage vector. The problem that the error range of voltage vector increases due to the large range of voltage vector is solved. Therefore, using DCF2 as the cost function for optimization will make the control system have better steady-state performance than DCF3.

(3) For DCF3, three groups of voltage vector combinations need to be screened from g_1, and then the optimal voltage vector is selected from the three groups of voltage vector combinations through g_2, which expands the screening range of DCF3 voltage vector combinations. Compared with DCF2, DCF3 can obtain the optimal voltage vector more accurately and further improve the dynamic performance of the motor. However, it increases the uncertainty of the weight balance between the optimal voltage vector and the number of switching changes, resulting in that although the stator current error of the optimal voltage vector decreases, the switching frequency increases, and the steady-state characteristics of the control system become worse.

The schematic diagram of DCF-MPC is shown in Figure 4.

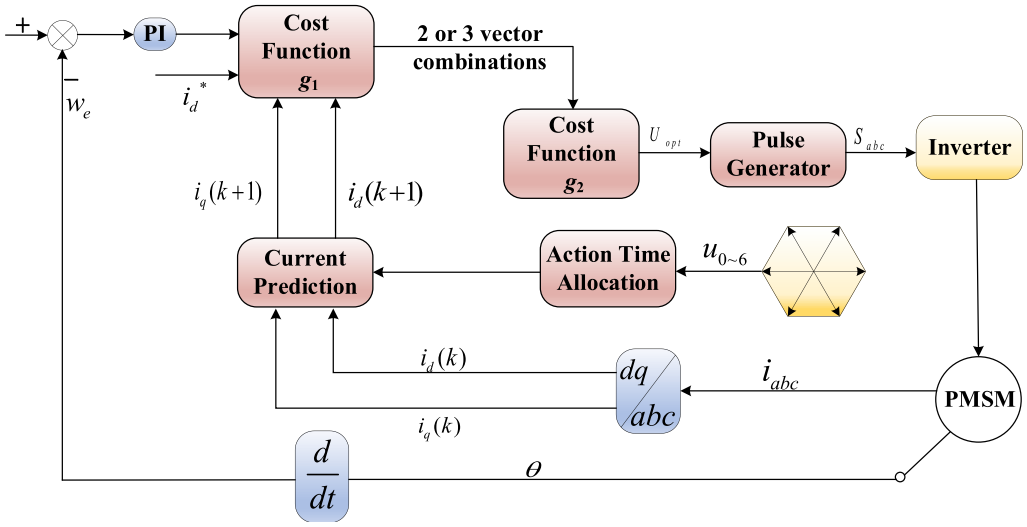

Figure 4. The schematic diagram of DCF-MPC.

5. EXPERIMENTAL VERIFICATION

To verify the correctness and effectiveness of the proposed method, the SCF-MPC with switching frequency is compared with the DCF-MPC proposed in this paper, and Simulink simulation model is built. The model is downloaded to RT-LAB (OP5600) to realize the hardware in the loop system of PMSM drive system. The controller adopts TMS320F2812, and the inverter and other parts are constructed by RT-LAB. Figure 5(a) shows the schematic diagram of RT-LAB hardware in the loop system, and Figure 5(b) shows the RT-LAB platform. The parameters of PMSM are shown in Table 2.

Three experimental groups are set up as follows: (i) Traditional SCF-MPC with weight factor. The optimal weight factor $\lambda = 0.1$ is obtained through extensive experiments. (ii) DCF2-MPC without

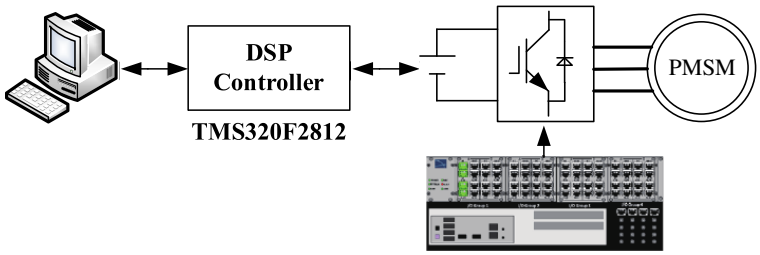

(a)

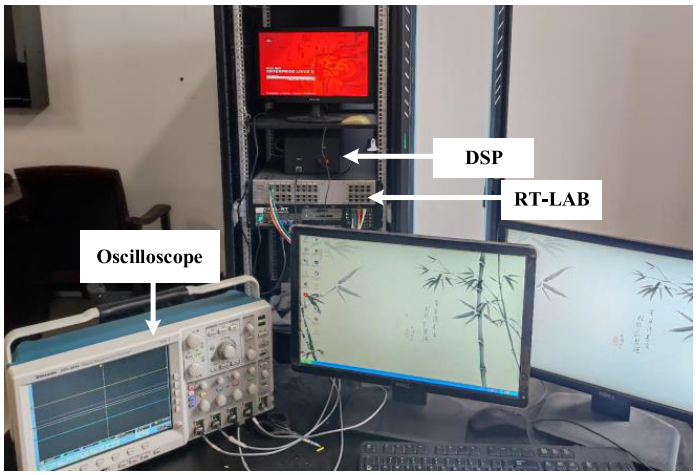

(b)

Figure 5. RT-LAB semi-physical experimental platform. (a) System in-the-loop configuration. (b) Semi-physical composition.

Table 2. Main parameters and values of PMSM.

Parameter	Value	Unit
Pole pairs	4	
Permanent magnet flux	0.24	Wb
Stator inductance	8.5	mH
Rated voltage	311	V
Rated current	9.4	A
Stator resistance	0.2	Ω
Rated speed	2000	r/min
Moment of inertia	0.00012	g·cm^2

weight factor. (iii) DCF3-MPC without weight factor. The PI parameters of the speed loop are the same for the three experimental groups, and the inner loop is FCS-MPC, $i_d^* = 0$. The dynamic performance, steady-state prediction error, and harmonic content of the three groups of experiments in the motor starting and dynamic process are verified.

Figure 6 shows the curve of no-load with a speed of 1000 r/min and a sudden load of 10 N·m at 0.1 s. It can be seen from Fig. 6 that the speed of DCF2-MPC and DCF3-MPC strategies under no-load almost has no overshoot, while SCF-MPC has 1% (10 r/min) overshoot. After the sudden load, the maximum current i_q peak in SCF-MPC is 8.87 A, and that in DCF3-MPC is 8.31 A. The current ripples of SCF-MPC and DCF3-MPC are 1.53 A and 1.37 A, respectively, while that of DCF2-MPC is 1.24 A. Compared with DCF3-MPC, the current ripple of DCF2-MPC decreases by 9.49%, while compared with SCF-MPC, its current ripple decreases by 18.95%. Therefore, DCF2-MPC has better effect in reducing current ripple. Under the same speed loop control, DCF2-MPC has stronger load carrying capacity and better steady-state characteristics.

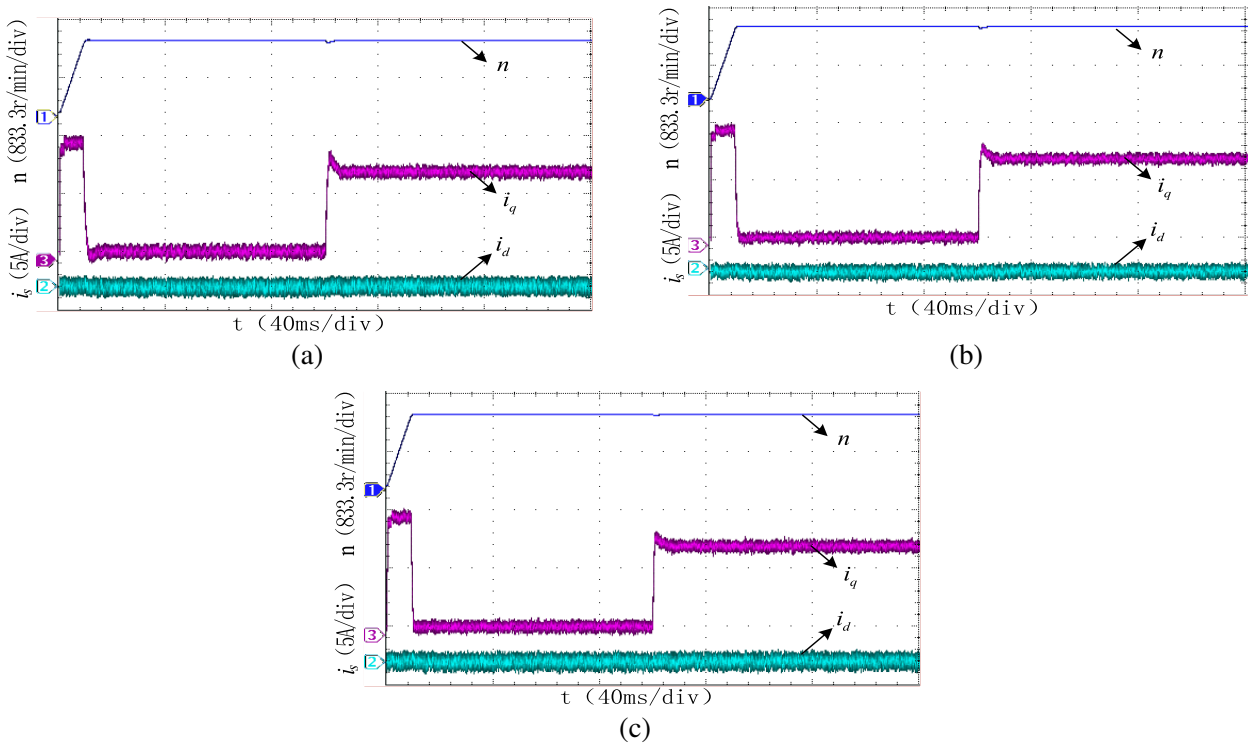

Figure 6. Motor speed and stator current waveforms. (a) SCF-MPC, (b) DCF2-MPC, (c) DCF3-MPC.

Phase current waveform and fast Fourier transform (FFT) analysis of i_a with 10 N·m load at 0.1 s are shown in Figure 7. The total harmonic distortion (THD) of SCF-MPC, DCF3-MPC, and DCF2-MPC are 4.57%, 4.9%, and 4.15%, respectively. Compared with SCF-MPC, the THD of DCF2-MPC decreases by 9.19%, while that of DCF3-MPC increases by 7.22%. The experimental results show that DCF2-MPC can reduce harmonic content, reduce current distortion, and improve waveform quality.

The given speed of the motor is 1000 r/min, and the load is suddenly increased by 10 N·m at 0.1 s. The speed is 1500 r/min at 0.2 s, and the speed is 500 r/min at 0.3 s. The speed waveforms of the three control strategies are shown in Figure 8. The adjustment time for acceleration is about 0.022 s, while the adjustment time for deceleration is about 0.012 s. The adjustment time of the three control strategies in acceleration and deceleration is almost different. Therefore, the three control strategies have the same speed response when the speed changes under the condition of constant load.

To further verify the performance of the three control strategies under different working conditions, the speed is 1000 r/min, and the load is 10 N·m at 0.1 s. The load is decreased from 10 N·m to 5 N·m at

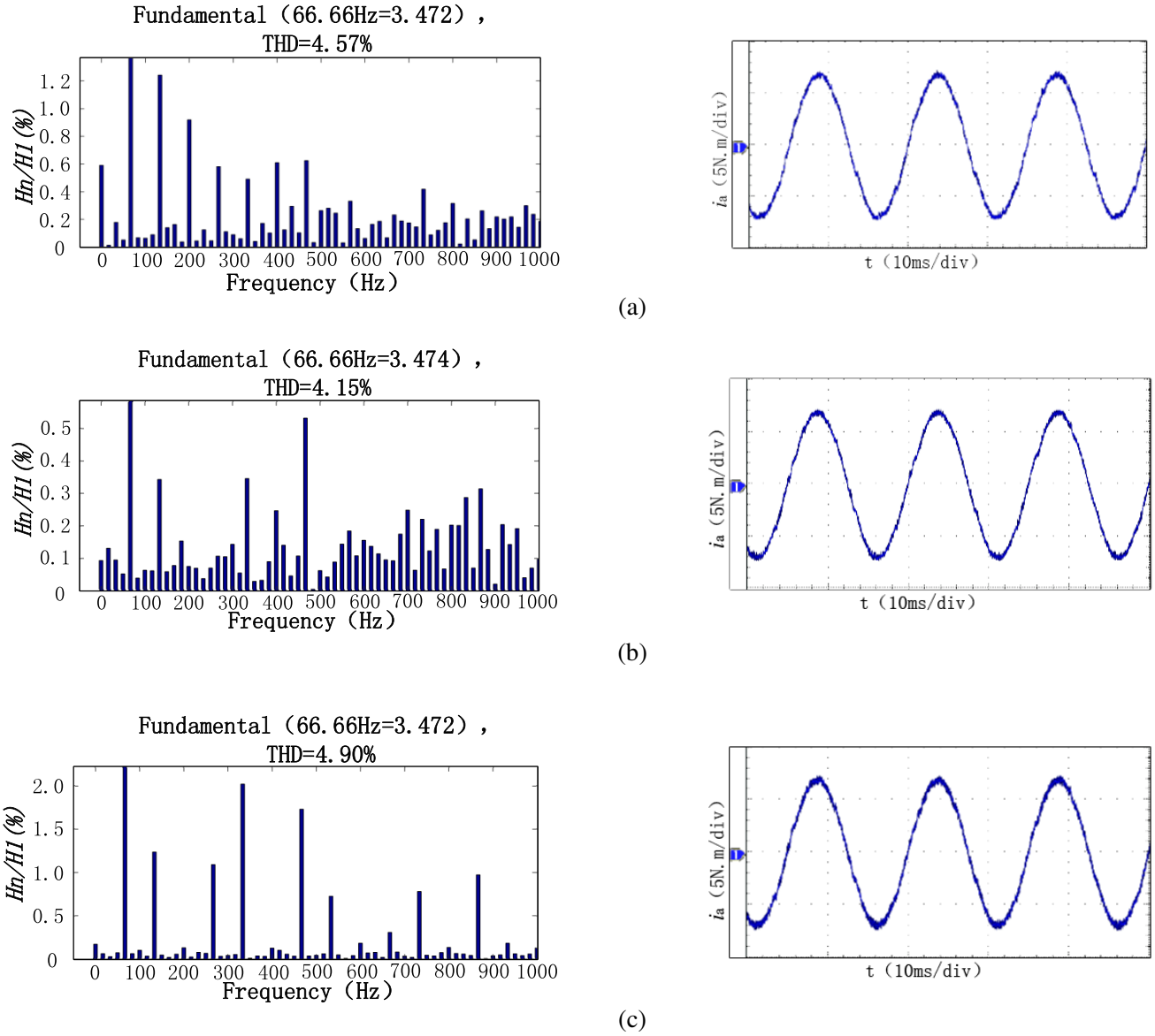

Figure 7. Phase current i_a waveform and FFT analysis. (a) SCF-MPC, (b) DCF2-MPC, (c) DCF3-MPC.

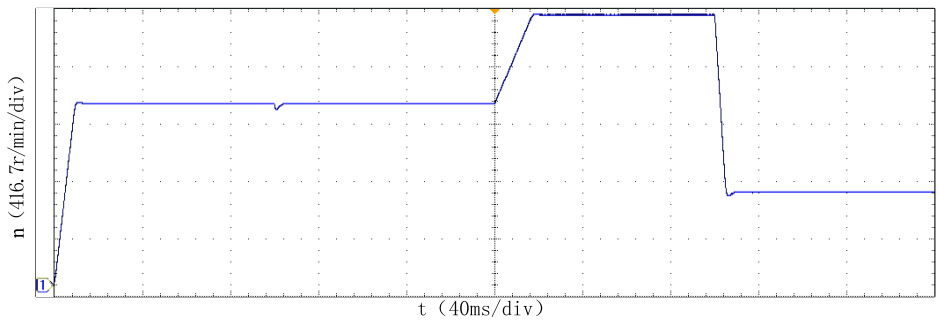

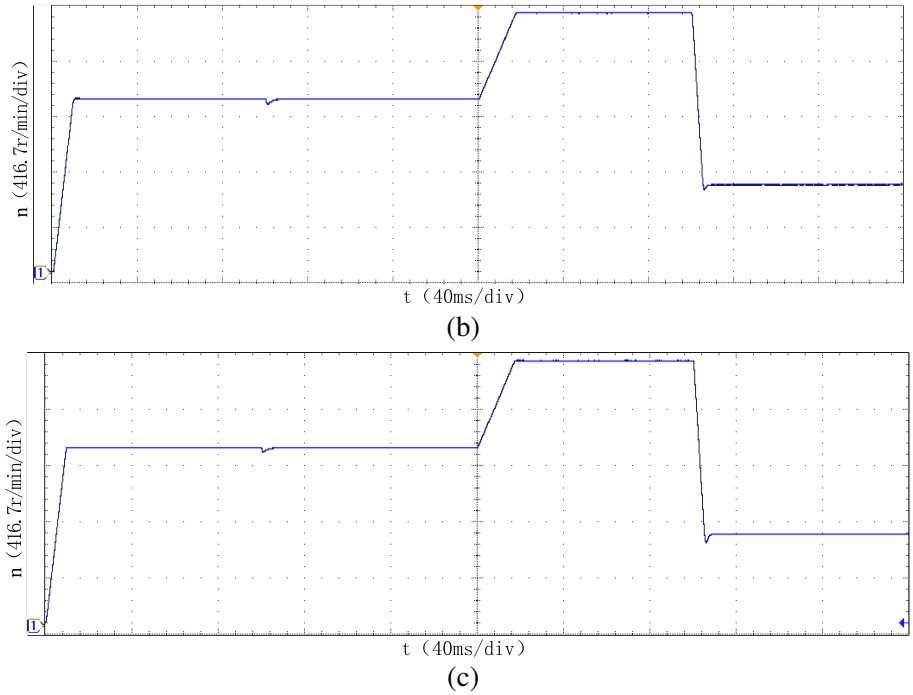

Figure 8. The speed waveforms of the three control strategies. (a) SCF-MPC, (b) DCF2-MPC, (c) DCF3-MPC.

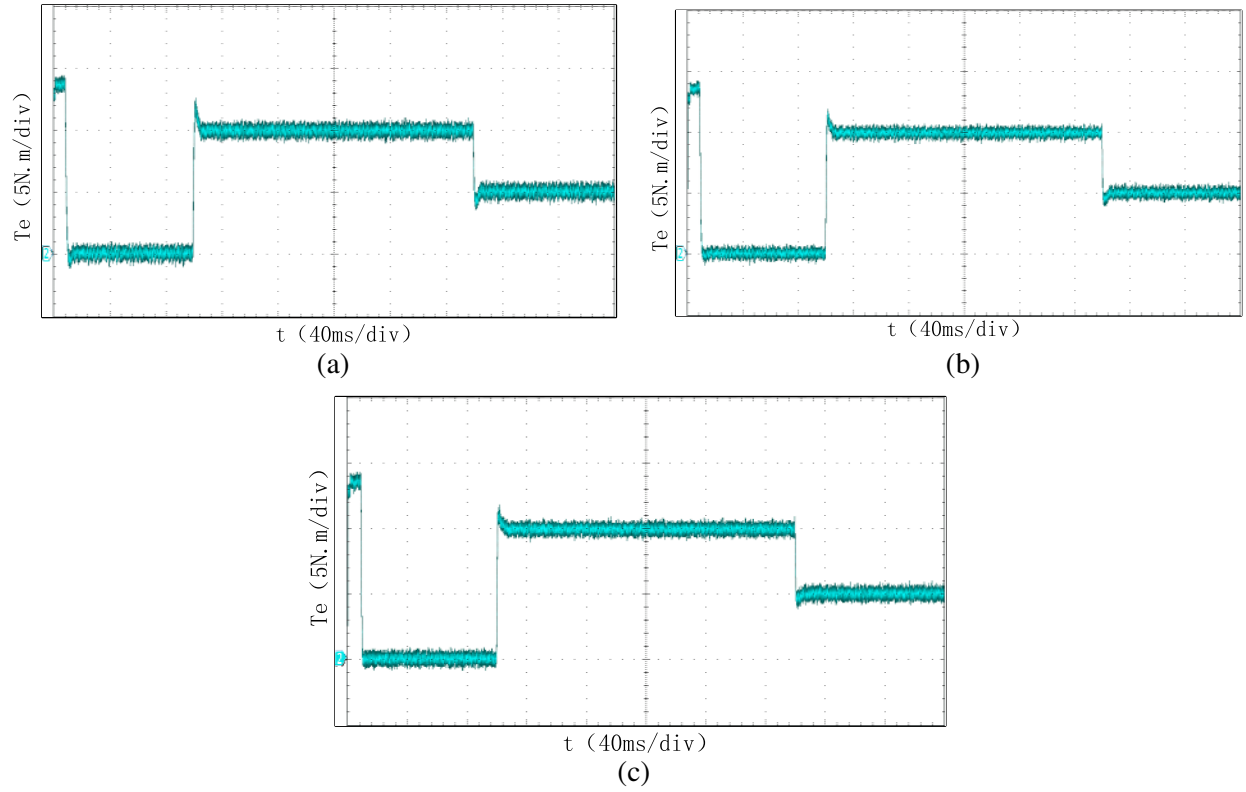

Figure 9. Torque waveform during loading and unloading. (a) SCF-MPC, (b) DCF2-MPC, (c) DCF3-MPC.

Table 3. T_e comparison of three control strategies.

	SCF-MPC	DCF3-MPC	DCF2-MPC
0.1 s δ (N·m)	2.533	1.71	2.024
0.3 s δ (N·m)	1.523	1.081	1.138
Δ (N·m)	0.787	0.713	0.654

0.3 s. The torque T_e change curve is shown in Figure 9. The experimental data are shown in Table 3 (δ represents the jitter value, and Δ represents the error value). Compared with SCF-MPC, the torque jitter δ of DCF2-MPC is reduced by 20.01% during loading and 5.28% during unloading. The torque ripple is reduced by 16.90%. The results show that DCF2-MPC obviously suppresses the torque ripple of the system during loading and unloading and has better anti-interference performance. Compared with SCF-MPC, the torque jitter δ of DCF3-MPC is reduced by 32.49% during loading and 29.02% during unloading. The torque ripple is only reduced by 9.40%. Although DCF2-MPC is not as effective as DCF3-MPC in restraining torque jitter, DCF2-MPC has obvious advantages in restraining ripple.

In conclusion, the experiment proves that DCF2-MPC not only has excellent dynamic performance, but also has optimal steady-state characteristics, so it is more suitable for practical application.

6. CONCLUSION

To solve the problem of complex weight factor adjustment caused by introducing switching frequency into the cost function of model predictive current control, the DCF method is proposed to avoid the weight factor. The stator current and switching frequency are designed as two cost functions to continuously select the optimal voltage vector. The following conclusions are drawn from experimental analysis:

(1) The proposed strategy eliminates the weight factor between current and switching frequency, and avoids the complex problem of weight factor design.

(2) The proposed strategy significantly reduces calculation burden. The SCF-MPC calculates the number of switching changes 21 times in a cycle, while the DCF2-MPC only needs to calculate 2 times.

(3) Compared with SCF-MPC, the THD of DCF2-MPC is reduced by 9.19%; the phase current harmonics are suppressed; the torque ripple is weakened; and the steady and dynamic performance of DCF2-MPC is better.

In this paper, the influence of motor parameter changes on the proposed method is not considered, and the next step will focus on this problem.

ACKNOWLEDGMENT

This work was supported by the Educational Commission of Hunan Province of China under Grant Number 21B0552.

REFERENCES

1. Yu, H., J. Wang, and Z. Xin, "Model predictive control for PMSM based on discrete space vector modulation with RLS parameter identification," *Energies*, Vol. 15, No. 11, 1–16, 2022.
2. Rodriguez, J., J. Pontt, C. A. Silva, et al., "Predictive current control of a voltage source inverter," *IEEE Transactions on Industrial Electronics*, Vol. 54, No. 1, 495–503, 2007.
3. Lyu, Z., X. Wu, J. Gao, et al., "An improved finite-control-set model predictive current control for IPMSM under model parameter mismatches," *Energies*, Vol. 14, No. 19, 1–13, 2021.

4. Uddin, M. and M. Rahman, "Online torque-flux estimation-based nonlinear torque and flux control scheme of IPMSM drive for reduced torque ripples," *IEEE Transactions on Power Electronics*, Vol. 34, No. 1, 636–645, 2019.
5. Pak, S. and I. Kang, "Sensorless vector control of permanent magnetic synchronous motor with parameter error compensation," *International Transactions on Electrical Energy Systems*, Vol. 31, No. 5, e12787, 2021.
6. Xia, C., J. Zhao, Y. Yan, et al., "A novel direct torque control of matrix converter fed PMSM drives using duty cycle control for torque ripple reduction," *IEEE Transactions on Industrial Electronics*, Vol. 61, No. 6, 2700–2713, 2013.
7. Yao, X., C. Huang, J. Wang, et al., "Predictive current control of dual vector model of permanent magnet synchronous motor with parameter identification function," *Proceedings of the CSEE*, 1–13, 2022.
8. Zhang, Y., J. Zhu, and W. Xu, "Predictive torque control of permanent magnet synchronous motor drive with reduced switching frequency," *2010 International Conference on Electrical Machines and Systems*, 798–803, 2010.
9. Yao, J., R. Liu, and X. Yin, "Research on predictive control of three-vector low switching frequency model of permanent magnet synchronous motor," *Transactions of China Electrotechnical Society*, Vol. 33, No. 13, 2935–2945, 2018.
10. Habibullah, M., D. Lu, D. Xiao, et al., "Predictive torque control of induction motor sensorless drive fed by a 3L-NPC inverter," *IEEE Transactions on Industrial Informatics*, Vol. 13, No. 1, 60–70, 2016.
11. Zhang, Z., Y. Liu, J. Chen, et al., "Predictive control strategy of permanent magnet synchronous motor amplitude control set model," *Transactions of China Electrotechnical Society*, Vol. 37, No. 23, 6126–6134, 2022.
12. Tu, W., G. Luo, and W. Liu, "Prediction of current control by finite control set model of permanent magnet synchronous motor based on fuzzy dynamic cost function," *Transactions of China Electrotechnical Society*, Vol. 32, No. 16, 89–97, 2017.
13. Li, J., F. Wang, D. Ke, et al.,"Design of predictive control weight coefficient of permanent magnet synchronous motor model based on particle swarm algorithm," *Transactions of China Electrotechnical Society*, Vol. 36, No. 1, 50–59+76, 2021.
14. Novak, M., H. Xie, T. Dragicevic, et al., "Optimal cost function parameter design in predictive torque control (PTC) using artificial neural networks (ANN)," *IEEE Transactions on Industrial Electronics*, Vol. 68, No. 8, 7309–7319, 2021.
15. Abbaszadeh, A., D. Khaburi, H. Mahmoudi, et al., "Simplified model predictive control with variable weighting factor for current ripple reduction," *IET Power Electronics*, Vol. 10, No. 10, 1165–1174, 2017.
16. Liu, X., D. Wang, and Z. Peng, "Cascade-free fuzzy finite-control-set model predictive control for nested neutral point-clamped converters with low switching frequency," *IEEE Transactions on Control Systems Technology*, Vol. 27, No. 5, 2237–2244, 2019.
17. Guazzelli, P., W. de Andrade Pereira, C. de Oliveira, et al., "Weighting factors optimization of predictive torque control of induction motor by multi-objective genetic algorithm," *IEEE Transactions on Power Electronics*, Vol. 34, No. 7, 6628–6638, 2018.
18. Caseiro, L., A. Mendes, and S. Cruz, "Dynamically weighted optimal switching vector model predictive control of power converters," *IEEE Transactions on Industrial Electronics*, Vol. 66, No. 2, 1235–1245, 2019.
19. Wang, F., J. Li, Z, Li, et al., "Design of model predictive control weighting factors for PMSM using gaussian distribution-based particle swarm optimization," *IEEE Transactions on Industrial Electronics*, Vol. 69, No. 11, 10935–10946, 2022.
20. Rojas, C., J. Rodriguez, F. Villarroel, et al., "Predictive torque and flux control without weighting factors," *IEEE Transactions on Industrial Electronics*, Vol. 60, No. 2, 681–690, 2012.

21. Xu, Y., Y. He, and S. Li, "Logical operation-based model predictive control for quasi-Z-source inverter without weighting factor," *IEEE Journal of Emerging and Selected Topics in Power Electronics*, Vol. 9, No. 1, 1039–1051, 2021.
22. Zhang, Y. and H. Yang, "Two-vector-based model predictive torque control without weighting factors for induction motor drives," *IEEE Transactions on Power Electronics*, Vol. 31, No. 2, 1381–1390, 2016.
23. Zhang, Y., H. Yang, and B. Xia, "Model-predictive control of induction motor drives: Torque control versus flux control," *IEEE Transactions on Industry Applications*, Vol. 52, No. 5, 4050–4060, 2016.
24. Wang, F., H. Xie, Q. Chen, et al., "Parallel predictive torque control for induction machines without weighting factors," *IEEE Transactions on Power Electronics*, Vol. 35, No. 2, 1779–1788, 2020.
25. Liu, J., Z. Ge, X. Wu, et al., "Predictive current control of permanent magnet synchronous motor based on duty cycle modulation," *Proceedings of the CSEE*, Vol. 40, No. 10, 3319–3328, 2020.